DINAME 2023 - Proceedings of the XIX International Symposium on Dynamic Problems of Mechanics,
A.S. De Paula, A.T. Fabro and M.R. Machado (Editors), ABCM.
Pirenópolis, Go, Brazil, February 26th to March 3rd, 2023

Protecting vibration-sensitive structures against ground vibration via the installation of heavy walls

David Carneiro[1], **Leonardo Antoniazzi Marques**[2], **and Josué Labaki**[2]

[1] KU Leuven, Dept. of Civil Eng., Structural Mech. Section, Kasteelpark Arenberg 40 box 2448, 3001 Leuven, Belgium

[2] School of Mechanical Engineering, University of Campinas. 200 Mendeleyev St, Campinas SP Brazil

Abstract: This paper investigates the ground vibration attenuation performance of heavy walls, in terms of their ability to reduce vibration levels of target structures. The analysis is focused on the problem of ground vibration generated by time-harmonic loads applied at an infinitely long rigid base. The target structure and the wall are modeled as prismatic, elastic bodies. The analysis uses a coupled IBEM-FEM scheme to model the dynamic wall–soil–structure interaction, which uses the classical Finite Element Method (FEM) to model the structure and the wall, and the Indirect Boundary Element Method (IBEM) to model the soil. The results show that the wall is able to provide significant reduction of the vibration levels of the target structure at specific frequencies, and that the wall can be designed to induce this reduction at desired frequencies.

Keywords: Ground vibration, vibration attenuation, gabion walls, coupled methods

INTRODUCTION

Road and railway traffic are a major source of ground vibration in urban areas. Railway-induced vibration, in particular, are a considerable inconvenience in residential neighborhoods. Urban developers resort to a number of technical solutions to mitigate this problem, among which is the installation of walls between the train tracks and the structures to be protected against vibration. These walls can be stone and masonry walls, stacks of interlocking concrete blocks, or even simple gabion walls, which are comparatively inexpensive to install and maintain.

The effectiveness of walls in mitigating ground vibration has been studied by various authors. The interest in this problem can be traced back to Krylov (2007), who proposed that heavy bodies such as decorative roadside boulders could be used to attenuate ground vibration generated by road traffic. He showed that part of the energy from the ground vibration impinging onto the boulders is used to induce motion of the boulder, resulting in partial attenuation of the incoming vibration. This argument was later confirmed by experimental results conducted by Mhanna et al. (2014) and Masoumi et al. (2014), among others. Dijckmans et al. (2015) used a numerical model and experimental results to show, additionally, that the attenuation provided by surface walls is connected to the vibration modes of the surface structures. This indicates that material and geometric properties of walls could be selected to induce maximum attenuation at a desired frequency of ground vibration. More recently, Carneiro et al. (2022) provided additional details on the mechanisms by which walls attenuate ground vibration. They showed that the wall converts part of the energy from surface waves into body waves, which are injected back into the bulk of the soil. Based on the time-harmonic model proposed by Carneiro et al. (2022), Marques and Labaki (2022) used a Fast Fourier Transform technique to analyze this problem for transient excitations, which are common in seismic excitation problems. They showed that, regardless of their vibration modes, walls provide significant attenuation of the most energy-carrying transient wavefront.

These previous studies, however, are focused on determining the effectiveness of the wall in attenuating vibration at the insertion point – the point where the wall is installed on the soil – or at discrete points behind the wall. The performance of the wall in attenuating vibration at a target structure that is installed behind it is not fully understood. It is well-established that the wall is able to attenuate vibrations at discrete points behind it. However, the intricacies of the dynamic interaction between a target structure and a continuous surface of the soil with which it interacts may play a significant role in this phenomenon. This is the question that is considered in this article. In view of the long length of gabion walls, the system is modeled in this paper as a two-dimensional, plane-strain problem.

Problem statement

Consider an infinitely long, rigid massless raft of width a on the surface of the soil, on which vertical ($z-$direction) time-harmonic loads F of circular frequency ω are applied (Fig. 1). At a distance d_w from this excitation source lies an infinitely long, linear-elastic wall of height H_w, width L_w, Young's modulus E_w, Poisson ratio ν_w, and mass density ρ_w. At a distance d_t from the wall lies an infinitely long, linear-elastic prismatic structure of height H_t, width L_t, Young's modulus E_t, Poisson ratio ν_t, and mass density ρ_t, referred to in this paper as "target" structure, because it is the structure for whose protection the wall is installed. The wall and the target structure are in perfectly bonded contact with the surface the soil, which is modeled as a linear-elastic, homogeneous, isotropic half-plane with Young's modulus E, Poisson ratio

ν, and mass density ρ. The problem consists in investigating the effect of the presence of the wall on the magnitude of vibration of the target structure.

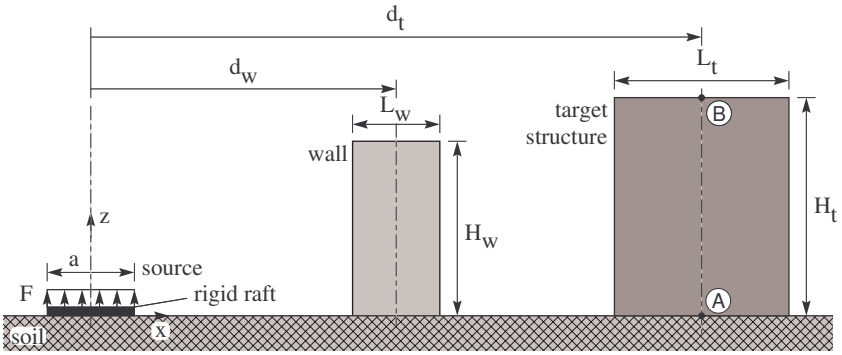

Figure 1 – Model of excitation source, wall, and target structure considered in this paper.

NUMERICAL MODEL

In order to provide an accurate representation of the wave propagation in the unbounded soil medium involved in this problem and of the energy exchanged between the structures on its surface, this paper uses a coupled model, involving classical finite element discretizations to represent the loaded raft, the wall, and the target structure, and a boundary element approach to represent the soil as an unbounded, wave-propagating medium.

Model of the soil

In this paper, the soil is modeled as a two-dimensional, linear-elastic, isotropic, homogeneous half-plane. The impedance of the soil at its contact surface with the structures can be obtained via the superposition of soil displacement influence functions, in the framework of the Indirect Boundary Element Method (IBEM). Solutions for these influence functions for the soil medium in this paper were available in the literature (Rajapakse and Wang, 1991), and are expressed in terms of improper integrals that can be evaluated numerically. A detailed description of the influence functions used in this paper, together with strategies for their numerical evaluation, can be found in Carneiro et al. (2022).

Model of the structures

In this section, we use the term "structures" to refer to the wall and the target structure, but also to the rigid raft where the loads are applied. The raft is also modeled as an elastic structure, only with a much higher Young's modulus than the rest of the system, so that it behaves as a rigid raft. The three structures in the system are modeled with classical finite elements. Four-noded quadrilateral elements with two displacement degrees of freedom per node are used. The equation of motion for each structure can be expressed as $\bar{\mathbf{K}}\mathbf{u} = \mathbf{f}$, in which $\bar{\mathbf{K}} = \mathbf{K} - \omega^2\mathbf{M}$ is the dynamic stiffness matrix of the structure, and $\mathbf{u}$ and $\mathbf{f}$ are the vectors of nodal displacements and forces.

Soil–structure coupling

The effect of the presence of the soil in the equation of motion of the structures is included via the incorporation of contact forces $\mathbf{f}_s$ as $\bar{\mathbf{K}}'\mathbf{u}' = \mathbf{f}' - \mathbf{f}_s$, in which the apostrophe denotes quantities referring to the nodes at the soil–structure interface.

The contact forces $\mathbf{f}_s$ at the interface nodes of the structures can be written in terms of soil contact forces. In this model, these unknown contact forces are approximated by piece-wise constant fictitious tractions $\mathbf{q}$. These can be written in terms of $\mathbf{f}_s$ as $\mathbf{f}_s = \mathbf{A}\mathbf{q}$, in which $\mathbf{A}$ is a purely geometric transformation matrix. In view of this transformation, the equation of motion can be rewritten as $\bar{\mathbf{K}}'\mathbf{u}' + \mathbf{A}\mathbf{q} = \mathbf{f}'$.

From the point of view of the soil, the application of fictitious contact tractions $\mathbf{q}$ at the soil–structure interface results in displacements on the soil surface that can be computed as $\mathbf{w}_s = \mathbf{U}\mathbf{q}$, in which $\mathbf{w}_s$ is the vector of nodal displacements of the soil at the interface. The influence matrix of the soil, $\mathbf{U}$, contains the soil influence functions described previously. These soil displacements $\mathbf{w}_s$ must hold continuity with respect to the displacements of the structures at the soil–structure interfaces, which can be stated as $\mathbf{w}_s = \mathbf{D}\mathbf{u}'$, in which $\mathbf{u}'$ is the vector of nodal displacements of the structure, and $\mathbf{D}$ is a purely geometric transformation matrix. This condition corresponds to the case in which the structures are in perfectly bonded contact with the soil, which is a reasonable assumption in this case in which heavy structures and low frequencies of excitation are considered. Displacements of the structures are therefore computed in terms of $\mathbf{q}$ as $\mathbf{D}\mathbf{u}' - \mathbf{U}\mathbf{q} = \mathbf{0}$. The expression of the transformation matrices $\mathbf{A}$ and $\mathbf{D}$ is given by Carneiro et al. (2022).

After some manipulation, the application of the equilibrium and continuity conditions at the interface between the soil and the three structures results in the equation of motion of the coupled system,

$$\begin{bmatrix} \bar{\mathbf{K}}_\mathbf{r} & \mathbf{0} & \mathbf{0} & \begin{Bmatrix} \mathbf{A_r} \\ \mathbf{0} \end{Bmatrix} & \mathbf{0} & \mathbf{0} \\ \mathbf{0} & \bar{\mathbf{K}}_\mathbf{w} & \mathbf{0} & \mathbf{0} & \begin{Bmatrix} \mathbf{A_w} \\ \mathbf{0} \end{Bmatrix} & \mathbf{0} \\ \mathbf{0} & \mathbf{0} & \bar{\mathbf{K}}_\mathbf{t} & \mathbf{0} & \mathbf{0} & \begin{Bmatrix} \mathbf{A_t} \\ \mathbf{0} \end{Bmatrix} \\ \begin{Bmatrix} \mathbf{D_r} & \mathbf{0} \end{Bmatrix} & \mathbf{0} & \mathbf{0} & -\mathbf{U_{rr}} & -\mathbf{U_{rw}} & -\mathbf{U_{rt}} \\ \mathbf{0} & \begin{Bmatrix} \mathbf{D_w} & \mathbf{0} \end{Bmatrix} & \mathbf{0} & -\mathbf{U_{wr}} & -\mathbf{U_{ww}} & -\mathbf{U_{wt}} \\ \mathbf{0} & \mathbf{0} & \begin{Bmatrix} \mathbf{D_t} & \mathbf{0} \end{Bmatrix} & -\mathbf{U_{tr}} & -\mathbf{U_{tw}} & -\mathbf{U_{tt}} \end{bmatrix} \begin{Bmatrix} \mathbf{u_r} \\ \mathbf{u_w} \\ \mathbf{u_t} \\ \mathbf{q_r} \\ \mathbf{q_w} \\ \mathbf{q_t} \end{Bmatrix} = \begin{Bmatrix} \mathbf{f_r} \\ \mathbf{f_w} \\ \mathbf{f_t} \\ \mathbf{0} \\ \mathbf{0} \\ \mathbf{0} \end{Bmatrix}, \quad (1)$$

in which $\bar{\mathbf{K}}_i$ is the dynamic stiffness matrix of structure i ($i = r$ denotes the raft, $i = w$ denotes the wall, and $i = t$ denotes the target structure), $\mathbf{A_i}$ and $\mathbf{D_i}$ denote the transformation matrices at the interface between the soil and structure i, $\mathbf{U_{ij}}$ ($j = r,w,t$) denotes influence matrices, describing displacements of boundary element nodes of the soil under structure i due to loads applied at boundary element nodes of the soil under structure j, $\mathbf{u_i}$ and $\mathbf{f_i}$ are nodal displacements and forces of structure i, and $\mathbf{q_i}$ are fictitious contact tractions at the interface between structure i and the soil. In this model, loads are only applied at the raft, so $\mathbf{f_w} = \mathbf{f_t} = \mathbf{0}$. Solving Eq. 1 for a set of external loads $\mathbf{f_r}$ results in the displacements of all structures.

NUMERICAL RESULTS

The results in this section consider the case of a typical gabion wall with $E_w = 367\,\text{MPa}$, $\nu_w = 0.2$, and $\rho_w = 1,700\,\text{kg/m}^3$, a target structure made of concrete with $E_t = 3,000\,\text{MPa}$, $\nu_t = 0.2$, and $\rho_t = 2,400\,\text{kg/m}^3$, and the soil with $E = 292\,\text{MPa}$, $\nu_w = 0.2$, and $\rho_w = 1,945\,\text{kg/m}^3$. The rigid raft has width $a = 1\,\text{m}$. The other dimensions are $d_t = 2d_w = 4\,\text{m}$, $H_w = H_t = 2\,\text{m}$, and $L_w = L_t = 1\,\text{m}$. Results are computed at points A (at the bottom of the target structure, $x = d_t, z = 0$; see Fig. 1) and B (at the top of the target structure, $x = d_t, z = H_t$), and presented in terms of the insertion loss $IL_i^p = 20\log_{10}(|u_i^b|/|u_i^a|)$, in which u_i denote displacements of the measured points in the $i-$direction, superscripts b and a indicate quantities measured before and after the installation of the wall, respectively, and $p = A,B$ indicate the point of measurement (Fig. 1). Positive and negative values of insertion loss indicate that the inclusion of the wall resulted in vibration attenuation and amplification on the measured point, respectively.

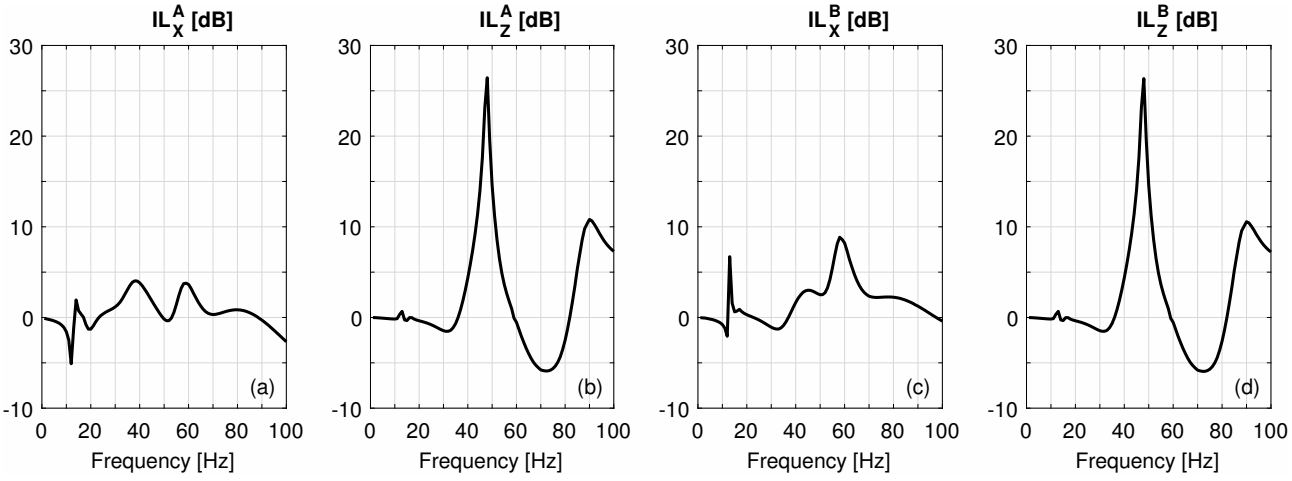

Figure 2 – Insertion loss at the bottom (a, b) and top (c, d) of the target structure.

Figure 2 shows that the wall is capable of providing significant vibration attenuation at both points of the target structure and in both directions of excitation. The attenuation is the most significant at specific frequencies of excitation, which are related to the vibration modes of the wall (Carneiro et al., 2022). This indicates that material and dimensions of the wall can be selected to provide maximum attenuation of motion of the target structure at specific frequencies of interest. Figure 3 shows a broader picture of the phenomenon. This case considers the same material parameters than the previous analysis, except that the target structure has the material properties of the gabion wall and $H_t = L_t = 10\,\text{m}$. A frequency of excitation of 53 Hz is considered, which is one of the natural frequencies of flexural vibration of the wall, in which the wall has been found to provide the maximum attenuation of ground vibration (Carneiro et al., 2022). The colormaps in Fig. 3[1] show the longitudinal strain in the $z-$direction, ε_{zz}. These strain fields in the soil are computed

[1]Figure 3 is an animated figure that is not being shown properly due to size limitations of this PDF. In order to see the animation, please click here.

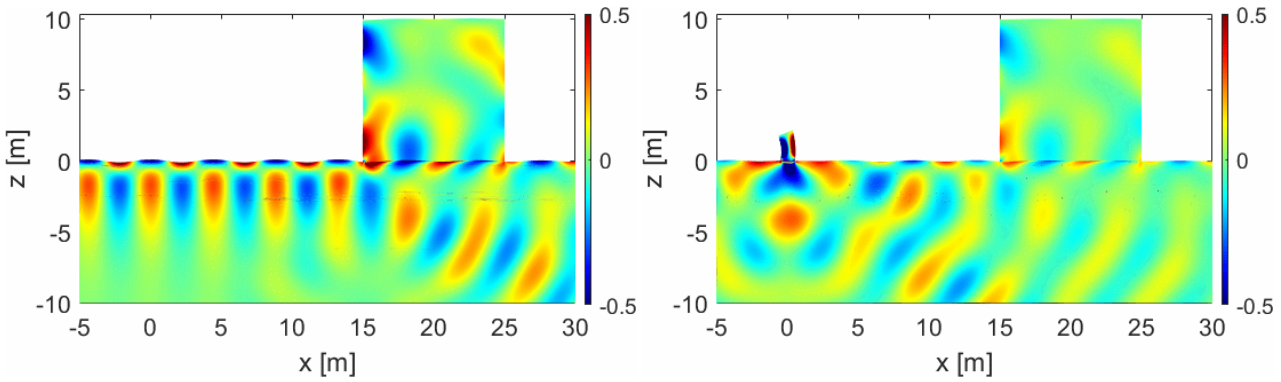

Figure 3 – Propagation of elastic waves in the soil and in the target structure a) without and b) with a gabion wall.

by post-processing from the fictitious contact tractions **q** from Eq. 1 (Carneiro et al., 2019). These results illustrate the mechanisms by which the wall attenuates ground vibration. Part of the energy carried by the surface wave is converted by the wall into body waves and injected into the bulk of the soil, and barred from reaching the target structure. An additional portion of the energy from the surface wave is converted into kinetic energy for the vibration of the wall itself. Alternating positive and negative values of strain on the two sides of the wall, indicating alternating expansion and compression, indicate that the wall is undergoing substantial flexural vibration. This is expected, since the wall is being excited at its natural frequency of flexural vibration, the energy for which is being withdrawn from the surface wave. As a result of these two mechanisms, the magnitude of the strain of the structure is significantly reduced after the installation of the wall, as indicated by the reduced intensity of the colors in the colormap, indicating reduction in the magnitude of strain.

CONCLUSIONS

This paper presented an analysis of the performance of heavy walls in protecting structures against time-harmonic ground vibration. A coupled IBEM-FEM method was used to model the problem. The source of excitation was described in terms of time-harmonic vertical loads applied to a rigid raft. Gabion walls and concrete target structures were selected to represent the analyzed system, in view of their applications in engineering practice. The results showed that the wall is capable of providing significant attenuation of the vibration of the target structure at specific frequencies. At the frequencies in which the attenuation provided by the wall is the most significant, vibration is attenuated in almost the entire body of the target structure. These results support the relatively inexpensive technology of heavy walls as viable devices for vibration attenuation in engineering practice.

REFERENCES

Carneiro, D., Barros, P. L. A., Labaki, J., 2022. "Ground vibration attenuation performance of surface walls". Computers and Geotechnics, 1:28.

Carneiro, D., Labaki, J., Hoefel, S. S., Barros, P. L. A. "Dynamic Displacement and Strain Fields within Trenched Soils: Post-Processing Quantities from Indirect-BEM's Fictitious Loads." In: Iberian Latin American Congress on Computational Methods in Engineering, CILAMCE 2019.

Dijckmans, A., Coulier, P., Jiang, J., Toward, M., Thompson, D., Degrande, G., Lombaert, G., 2015. "Mitigation of railway induced ground vibration by heavy masses next to the track." Soil Dynamics and Earthquake Engineering 75, 158–170.

Krylov, V. V., 2007. "Control of traffic-induced ground vibrations by placing heavy masses on the ground surface." Journal of low frequency noise, vibration and active control 26, 311–321.

Marques, L. A., Labaki, J. "A time-domain IBEM-FEM model of the ground vibration attenuation function of surface walls." In: 8th International Symposium on Solid Mechanics, Mecsol 2022.

Masoumi, H., Van Leuven, A., Urbaniak, S., 2014. "Mitigation of train induced vibrations by wave impeding blocks: numerical prediction and experimental validation." EURO5DYN 2014 , 863–870.

Mhanna, M., Shahrour, I., Sadek, M., Dunez, P., 2014. "Efficiency of heavy mass technology in traffic vibration reduction: Experimental and numerical investigation." Computers and Geotechnics 55, 141–149.

Rajapakse, R., Wang, Y., 1991. "Elastodynamic Green's functions of orthotropic half plane." Journal of engineering mechanics 117, 588–604.

RESPONSIBILITY NOTICE

The authors are the only parties responsible for the printed material included in this paper.